Detecting dark energy with wavelets on the sphere

Jason McEwen
http://www.mrao.cam.ac.uk/~jdm57/

Astrophysics Group, Cavendish Laboratory, University of Cambridge

SPIE Optics and Photonics 2007 :: Wavelets XII

Outline

Outline

Content of the Universe

- Universe consists of ordinary baryonic matter, cold dark matter and dark energy.
- Dark energy represents energy density of empty space. Modelled by a cosmological fluid with negative pressure acting as a repulsive force.
- Evidence for dark energy provided by observations of CMB, supernovae and large scale structure of Universe.

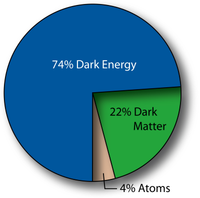

Credit: WMAP Science Team

- However, a consistent model in the framework of particle physics lacking. Indeed, atempts to predict a cosmological constant obtain a value that is too large by a factor of $\sim 10^{120}$.
- Dark energy dominates our Universe but yet we know very little about its nature and origin.
- Verification of dark energy by independent physical methods of considerable interest.
- Independent methods may also prove more sensitive probes of properties of dark energy.

Cosmic microwave background (CMB) radiation

- Temperature of early Universe sufficiently hot that photons had enough energy to ionise hydrogen.
- Compton scattering happened frequently $\Rightarrow$ mean free path of photons extremely small.
- Universe consisted of an opaque photon-baryon fluid.
- As Universe expanded it cooled, until majority of photons no longer had sufficient energy to ionise hydrogen.
- Photons decoupled from baryons and the Universe became essentially transparent to radiation.
- *Recombination* occurred when temperature of Universe dropped to 3000K ($\sim$400,000 years after the Big Bang).
- Photons then free to propagate largely unhindered and observed today on celestial sphere as CMB radiation.

WMAP3 ILC movie

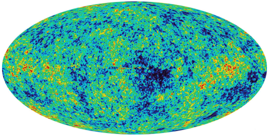

Integrated Sachs-Wolfe (ISW) effect

Ball sim

(a) Matter domination

Ball sim

(b) Deviation from matter domination

Figure: ISW effect analogy

- CMB photons blue (red) shifted when fall into (out of) potential wells
- Evolution of potential during photon propagation $\longrightarrow$ net change in photon energy
- Gravitation potentials constant w.r.t. conformal time in matter dominated universe
- Deviation from matter domination due to curvature or dark energy causes potentials to evolve with time $\longrightarrow$ secondary anisotropy induced in CMB

Integrated Sachs-Wolfe (ISW) effect

- WMAP shown universe is (nearly) flat
  detection of ISW effect $\longrightarrow$ direct evidence for dark energy
- Cannot isolate the ISW signal from CMB anisotropies easily
- Instead, detect by cross-correlating CMB anisotropies with tracers of large scale structure
  (Crittenden & Turok 1996 [4])
- Previous works
  - Real space angular correlation function
    (*e.g.* Boughn & Crittenden 2004 [3])
  - Harmonic space cross-angular power spectrum
    (*e.g.* Afshordi *et al.* 2004 [1])
  - Wavelet correlation
    (Vielva *et al.* 2005 [8]; McEwen *et al.* 2006 [6])
  - Morphological correlation
    (McEwen *et al.* 2007 [7])

Outline

1. Cosmology
   - Content of the Universe
   - Cosmic microwave background
   - Integrated Sachs-Wolfe effect
2. Wavelets on the sphere
   - Wavelet transform
   - Correspondence principle
   - Steerability
3. Detecting dark energy
   - Procedures
   - Data and simulations
   - Detections
4. Summary

Wavelet transform

- Follow construction derived by Antoine and Vandergheynst 1998 [2]. Reintroduced by Wiaux *et al.* 2005 [9] in an equivalent, practical and self-consistent approach.
- Construct wavelet basis from affine transformations (dilation, translation) on the sphere of a mother wavelet
- The natural extension of translations to the sphere are rotations. Characterised by the elements of the rotation group $\mathrm{SO}(3)$, which parameterise in terms of the three Euler angles $\rho = (\alpha, \beta, \gamma)$. Rotation of a function f on the sphere is defined by

$$[\mathcal{R}(\rho) f](\omega) = f(\rho^{-1}\omega), \quad \rho \in \mathrm{SO}(3) .$$

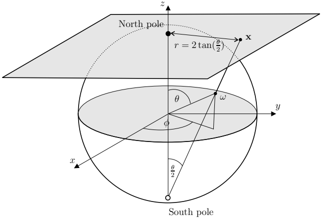

Figure: Stereographic projection

- The spherical dilation operator $\mathcal{D}(a, b)$ is defined as the conjugation by stereographic projection Π of the Euclidean dilation $d(a, b)$ in $\mathrm{L}^2(\mathbb{R}^2, \, \mathrm{d}^2\boldsymbol{x})$ on tangent plane at north pole:

$$\mathcal{D}(a, b) \equiv \Pi^{-1} \, d(a, b) \, \Pi .$$

- Although anisotropic dilations of practical use, not wavelets strictly speaking. In the anisotropic setting a bounded admissibility integral cannot be determined (even in the plane), thus the synthesis of a signal from its coefficients cannot be performed. For perfect reconstruction require $a = b$.

Wavelet transform

- **Wavelet basis** on the sphere may now be constructed from rotations and isotropic dilations of a mother spherical wavelet $\psi \in \mathrm{L}^2(\mathbb{S}^2)$. Corresponding wavelet family $\{\psi_{a,\rho} \equiv \mathcal{R}(\rho)\mathcal{D}(a,a)\psi : \rho \in \mathrm{SO}(3),\, a \in \mathbb{R}_*^+\}$ provides over-complete basis for $\mathrm{L}^2(\mathbb{S}^2)$.
- The **wavelet transform** of $f \in \mathrm{L}^2(\mathbb{S}^2)$ is given by the projection on to each wavelet basis function in the usual manner:

$$W_\psi^f(a,\rho) \equiv \int_{\mathbb{S}^2} \mathrm{d}\Omega(\omega)\, f(\omega)\, \psi_{a,\rho}^*(\omega) \;,$$

  where $\mathrm{d}\Omega(\omega) = \sin\theta \,\mathrm{d}\theta\,\mathrm{d}\varphi$ is the usual invariant measure on the sphere.
- **Fast algorithms** derived by McEwen *et al.* 2007 [5] and Wiaux *et al.* 2006 [10]

  - The **synthesis** of a signal on the sphere from its wavelet coefficients is given by

$$f(\omega) = \int_{\mathrm{SO}(3)} \mathrm{d}\varrho(\rho) \int_0^\infty \frac{\mathrm{d}a}{a^3}\, W_\psi^f(a,\rho)\, [\mathcal{R}(\rho) L_\psi \psi_a](\omega) \;,$$

    where $\mathrm{d}\varrho(\rho) = \sin\beta\,\mathrm{d}\alpha\,\mathrm{d}\beta\,\mathrm{d}\gamma$ is the invariant measure on the rotation group $\mathrm{SO}(3)$ and the L_ψ operator in $\mathrm{L}^2(\mathbb{S}^2)$ is defined by the action $(L_\psi g)_{\ell n} \equiv g_{\ell n}/C_\psi^\ell$ on the spherical harmonic coefficients of functions $g \in \mathrm{L}^2(\mathbb{S}^2)$.
  - In order to ensure the perfect reconstruction of a signal synthesised from its wavelet coefficients, one requires the **admissibility condition**

$$0 < C_\psi^\ell \equiv \frac{8\pi^2}{2\ell+1} \sum_{n=-\ell}^{\ell} \int_0^\infty \frac{\mathrm{d}a}{a^3} \mid (\psi_a)_{\ell n} \mid^2 < \infty$$

    to hold for all $\ell \in \mathbb{N}$, where $(\psi_a)_{\ell n}$ are the spherical harmonic coefficients of $\psi_a(\omega)$.

Wavelet transform

- Wavelet basis on the sphere may now be constructed from rotations and isotropic dilations of a mother spherical wavelet $\psi \in \mathrm{L}^2(\mathbb{S}^2)$. Corresponding wavelet family $\{\psi_{a,\rho} \equiv \mathcal{R}(\rho)\mathcal{D}(a,a)\psi : \rho \in \mathrm{SO}(3),\ a \in \mathbb{R}_*^+\}$ provides over-complete basis for $\mathrm{L}^2(\mathbb{S}^2)$.

- The wavelet transform of $f \in \mathrm{L}^2(\mathbb{S}^2)$ is given by the projection on to each wavelet basis function in the usual manner:

$$W_\psi^f(a,\rho) \equiv \int_{\mathbb{S}^2} \mathrm{d}\Omega(\omega)\, f(\omega)\, \psi_{a,\rho}^*(\omega) \ ,$$

  where $\mathrm{d}\Omega(\omega) = \sin\theta \,\mathrm{d}\theta\, \mathrm{d}\varphi$ is the usual invariant measure on the sphere.

- Fast algorithms derived by McEwen *et al.* 2007 [5] and Wiaux *et al.* 2006 [10]

  - The synthesis of a signal on the sphere from its wavelet coefficients is given by

$$f(\omega) = \int_{\mathrm{SO}(3)} \mathrm{d}\varrho(\rho) \int_0^\infty \frac{\mathrm{d}a}{a^3}\ W_\psi^f(a,\rho)\ [\mathcal{R}(\rho) L_\psi \psi_a](\omega) \ ,$$

    where $\mathrm{d}\varrho(\rho) = \sin\beta\, \mathrm{d}\alpha\, \mathrm{d}\beta\, \mathrm{d}\gamma$ is the invariant measure on the rotation group $\mathrm{SO}(3)$ and the L_ψ operator in $\mathrm{L}^2(\mathbb{S}^2)$ is defined by the action $(L_\psi g)_{\ell n} \equiv g_{\ell n}/C_\psi^\ell$ on the spherical harmonic coefficients of functions $g \in \mathrm{L}^2(\mathbb{S}^2)$.

  - In order to ensure the perfect reconstruction of a signal synthesised from its wavelet coefficients, one requires the admissibility condition

$$0 < C_\psi^\ell \equiv \frac{8\pi^2}{2\ell+1} \sum_{n=-\ell}^{\ell} \int_0^\infty \frac{\mathrm{d}a}{a^3}\ |\ (\psi_a)_{\ell n}\ |^2 < \infty$$

    to hold for all $\ell \in \mathbb{N}$, where $(\psi_a)_{\ell n}$ are the spherical harmonic coefficients of $\psi_a(\omega)$.

Correspondence principle

- Correspondence principle between spherical and Euclidean wavelets states that the inverse stereographic projection of an *admissible* wavelet on the plane yields an *admissible* wavelet on the sphere. (Proved by Wiaux *et al.* 2005 [9].)
- Mother wavelets on sphere constructed from the projection of mother Euclidean wavelets defined on the plane:

$$\psi(\omega) = [\Pi^{-1}\psi_{\mathbb{R}^2}](\omega) \ ,$$

  where $\psi_{\mathbb{R}^2} \in \mathrm{L}^2(\mathbb{R}^2, \, \mathrm{d}^2\boldsymbol{x})$ is an admissible wavelet in the plane.
- Directional wavelets on sphere may be naturally constructed in this setting – they are simply the projection of directional Euclidean planar wavelets on to the sphere.

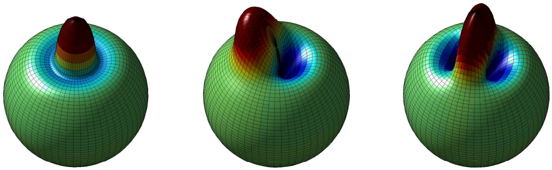

(a) SMHW (b) SBW (c) S2GDW

Figure: Spherical wavelets at scale $a = b = 0.2$.

Wavelet steerability

- Derived on the sphere by Wiaux *et al.* 2005 [9].
- For steerable wavelets, wavelet for any orientation γ given by weighted sum of basis wavelets:

$$\psi_\gamma(\omega) = \sum_{m=1}^{M} k_m(\gamma)\psi_m(\omega)$$

- Due to linearity of the wavelet transform, property extends to wavelet coefficients:

$$W^f_\psi(a,\alpha,\beta,\gamma) = \sum_{m=1}^{M} k_m(\gamma) W^f_{\psi_m}(a,\alpha,\beta,0)$$

Wavelet steerability

- Derived on the sphere by Wiaux *et al.* 2005 [9].
- For steerable wavelets, wavelet for any orientation γ given by weighted sum of basis wavelets:

$$\psi_\gamma(\omega) = \sum_{m=1}^{M} k_m(\gamma)\psi_m(\omega)$$

- Due to linearity of the wavelet transform, property extends to wavelet coefficients:

$$W_\psi^f(a, \alpha, \beta, \gamma) = \sum_{m=1}^{M} k_m(\gamma) W_{\psi_m}^f(a, \alpha, \beta, 0)$$

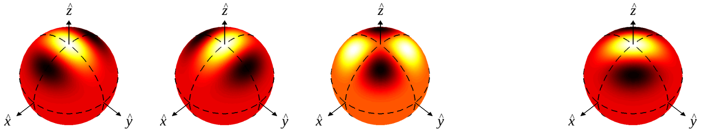

(a) $\Psi^{\partial_{\hat{x}}^2(Gauss)}$ (b) $\Psi^{\partial_{\hat{y}}^2(Gauss)}$ (c) $\Psi^{\partial_{\hat{x}}\partial_{\hat{y}}(Gauss)}$ (d) $\Psi^{\partial_{\hat{x}}^2(Gauss)}$ rotated by $\chi = \pi/4$

Figure: Second Gaussian derivative wavelet on the sphere for $a = 0.4$. The rotated wavelet illustrated in panel (d) can be constructed from a sum of weighted versions of the basis wavelets illustrated in panels (a) through (c). (Credit: Wiaux *et al.* 2005 [9])

Wavelet steerability

- Derived on the sphere by Wiaux *et al.* 2005 [9].
- For steerable wavelets, wavelet for any orientation γ given by weighted sum of basis wavelets:

$$\psi_\gamma(\omega) = \sum_{m=1}^{M} k_m(\gamma)\psi_m(\omega)$$

- Due to linearity of the wavelet transform, property extends to wavelet coefficients:

$$W^f_\psi(a, \alpha, \beta, \gamma) = \sum_{m=1}^{M} k_m(\gamma) W^f_{\psi_m}(a, \alpha, \beta, 0)$$

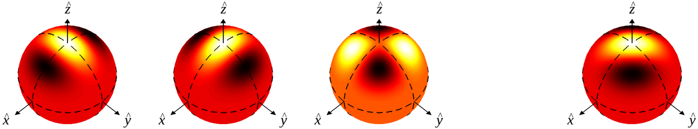

(a) $\Psi^{\partial^2_{\hat{x}}}(Gauss)$ (b) $\Psi^{\partial^2_{\hat{y}}}(Gauss)$ (c) $\Psi^{\partial_{\hat{x}}\partial_{\hat{y}}}(Gauss)$ (d) $\Psi^{\partial^2_{\hat{x}}}(Gauss)$ rotated by $\chi = \pi/4$

Figure: Second Gaussian derivative wavelet on the sphere for $a = 0.4$. The rotated wavelet illustrated in panel (d) can be constructed from a sum of weighted versions of the basis wavelets illustrated in panels (a) through (c). (Credit: Wiaux *et al.* 2005 [9])

Morphological measures

- Steerability may be used to compute measures of the morphology of local features.
- Orientation $D(\omega, a)$: Orientation of feature of maximum wavelet coefficient at each position on the sphere
- Signed-intensity $I(\omega, a)$: Maximum wavelet coefficient at given orientation
- Elongation $E(\omega, a)$: Unity minus ratio of wavelet coefficient in orthogonal direction relative to maximum wavelet coefficient

Outline

Procedures

- Wavelets ideal analysis tool to search for correlation induced by ISW effect
- Compute correlation in wavelet space (pioneered by Vielva *et al.* 2005 [8])
- Extend to a directional analysis (McEwen *et al.* 2006 [6])
- Correlate morphological measures (McEwen *et al.* 2007 [7])
- Acknowledgements: Patricio Vielva, Enrique Martínez-González, Yves Wiaux, Pierre Vandergheynst, Mike Hobson & Anthony Lasenby
- Correlate various measures:

$$X_{S_i}^{\mathrm{NT}}(a) = \frac{1}{N_{\mathrm{p}}} \sum_{\omega_0} S_i^{\mathrm{N}}(\omega_0, a)\, S_i^{\mathrm{T}}(\omega_0, a) - \bar{S}_i^{\mathrm{N}}(a)\, \bar{S}_i^{\mathrm{T}}(a)\ ,$$

  where $S_i = \{W,\ I,\ D,\ E\}$ and the bar denotes a mean.
- Three procedures:
  - Wavelet coefficient correlation
  - Local morphological correlation
  - Matched intensity correlation
- In absence of ISW effect don't expect to observe a significant correlation in any of these measures.

Procedures

- Wavelets ideal analysis tool to search for correlation induced by ISW effect
- Compute correlation in wavelet space (pioneered by Vielva *et al.* 2005 [8])
- Extend to a directional analysis (McEwen *et al.* 2006 [6])
- Correlate morphological measures (McEwen *et al.* 2007 [7])
- Acknowledgements: Patricio Vielva, Enrique Martínez-González, Yves Wiaux, Pierre Vandergheynst, Mike Hobson & Anthony Lasenby
- Correlate various measures:

$$X^{\mathrm{NT}}_{S_i}(a) = \frac{1}{N_{\mathrm{p}}} \sum_{\omega_0} S^{\mathrm{N}}_i(\omega_0, a)\, S^{\mathrm{T}}_i(\omega_0, a) - \bar{S}^{\mathrm{N}}_i(a)\, \bar{S}^{\mathrm{T}}_i(a) \ ,$$

  where $S_i = \{W,\ I,\ D,\ E\}$ and the bar denotes a mean.
- Three procedures:
  - Wavelet coefficient correlation
  - Local morphological correlation
  - Matched intensity correlation
- In absence of ISW effect don't expect to observe a significant correlation in any of these measures.

Procedures

- Wavelets ideal analysis tool to search for correlation induced by ISW effect
- Compute correlation in wavelet space (pioneered by Vielva *et al.* 2005 [8])
- Extend to a directional analysis (McEwen *et al.* 2006 [6])
- Correlate morphological measures (McEwen *et al.* 2007 [7])
- Acknowledgements: Patricio Vielva, Enrique Martínez-González, Yves Wiaux, Pierre Vandergheynst, Mike Hobson & Anthony Lasenby
- Correlate various measures:

$$X_{S_i}^{\mathrm{NT}}(a) = \frac{1}{N_{\mathrm{p}}} \sum_{\omega_0} S_i^{\mathrm{N}}(\omega_0, a)\, S_i^{\mathrm{T}}(\omega_0, a) - \bar{S}_i^{\mathrm{N}}(a)\, \bar{S}_i^{\mathrm{T}}(a) \ ,$$

  where $S_i = \{W,\ I,\ D,\ E\}$ and the bar denotes a mean.
- Three procedures:
  - Wavelet coefficient correlation
  - Local morphological correlation
  - Matched intensity correlation
- In absence of ISW effect don't expect to observe a significant correlation in any of these measures.

Procedures

- Wavelets ideal analysis tool to search for correlation induced by ISW effect
- Compute correlation in wavelet space (pioneered by Vielva *et al.* 2005 [8])
- Extend to a directional analysis (McEwen *et al.* 2006 [6])
- Correlate morphological measures (McEwen *et al.* 2007 [7])
- Acknowledgements: Patricio Vielva, Enrique Martínez-González, Yves Wiaux, Pierre Vandergheynst, Mike Hobson & Anthony Lasenby
- Correlate various measures:

$$X^{\mathrm{NT}}_{S_i}(a) = \frac{1}{N_{\mathrm{p}}} \sum_{\omega_0} S^{\mathrm{N}}_i(\omega_0, a)\, S^{\mathrm{T}}_i(\omega_0, a) - \bar{S}^{\mathrm{N}}_i(a)\, \bar{S}^{\mathrm{T}}_i(a) \;,$$

  where $S_i = \{W,\ I,\ D,\ E\}$ and the bar denotes a mean.
- Three procedures:
  - Wavelet coefficient correlation
  - Local morphological correlation
  - Matched intensity correlation
- In absence of ISW effect don't expect to observe a significant correlation in any of these measures.

Data and simulations

- Compute correlation from WMAP three-year CMB data and NVSS radio galaxy survey data
- Perform 1000 Monte Carlo simulations to quantify significance of any detections of correlation

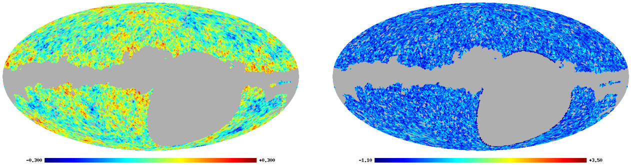

(a) WMAP (b) NVSS

Figure: WMAP co-added three-year and NVSS maps after application of the joint mask. The maps are downsampled to a pixel size of $\sim 55'$.

Detections: Wavelet coefficient correlation

- Distribution of wavelet correlation statistics found to be approximately Gaussian distributed $\Rightarrow$ approximate significance of detections of correlation may be inferred from number of standard deviations detection deviates from Monte Carlo simulations
- Anisotropic dilations adopted in this analysis.
- For both SMHW and SBW maximum correlation detected at $N_\sigma \simeq 3.9$ on wavelet scales about $\boldsymbol{a} = (100, 300)^{\mathrm{T}}$ arcminutes.
- Foreground contamination and instrumental systematics ruled out as source of the correlation $\Rightarrow$ correlation due to ISW effect

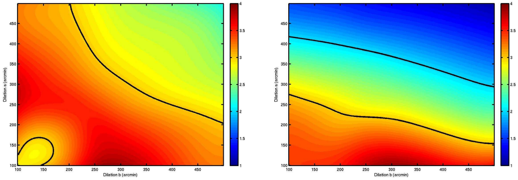

(a) SMHW (b) SBW

Figure: Wavelet correlation N_σ surfaces. Contours are shown for levels of two and three N_σ.

Detections: Wavelet coefficient correlation

- Possible to use positive detection of the ISW effect to constrain parameters of cosmological models that describe dark energy:
  - Proportional energy density Ω_Λ.
  - Equation of state parameter w relating pressure and density of cosmological fluid that mdoels dark energy, *i.e.* $p = w\rho$.
- Results shown for SMHW only (similar findings for SBW)
- Parameter estimates of $\Omega_\Lambda = 0.63^{+0.18}_{-0.17}$ and $w = -0.77^{+0.35}_{-0.36}$ computed from the mean of the marginalised distributions (consistent with other analysis techniques and data sets).

Detections: Wavelet coefficient correlation

- Possible to use positive detection of the ISW effect to constrain parameters of cosmological models that describe dark energy:
  - Proportional energy density Ω_Λ.
  - Equation of state parameter w relating pressure and density of cosmological fluid that mdoels dark energy, *i.e.* $p = w\rho$.
- Results shown for SMHW only (similar findings for SBW)
- Parameter estimates of $\Omega_\Lambda = 0.63^{+0.18}_{-0.17}$ and $w = -0.77^{+0.35}_{-0.36}$ computed from the mean of the marginalised distributions (consistent with other analysis techniques and data sets).

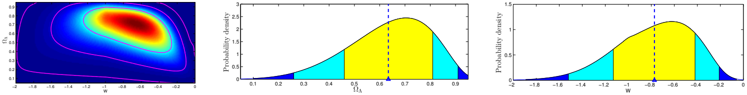

(a) Full likelihood surface (b) Marginalised distribution for Ω_Λ (c) Marginalised distribution for w

Figure: Likelihoods constructed using the SMHW for parameters (Ω_Λ, w). The full likelihood surface is shown in panel (a), with 68%, 95% and 99% confidence contours also shown. Marginalised distributions for each parameter are shown in the remaining panels, with 68% (yellow), 95% (light-blue) and 99% (dark-blue) confidence regions also shown. The parameter estimates made from the mean of the marginalised distribution are shown by the dashed line.

Detections: Local morphological correlation

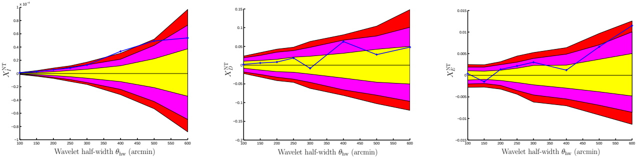

(a) Signed-intensity (b) Orientation (c) Elongation

Figure: Correlation statistics computed for each morphological measure in the local morphological analysis, from the WMAP co-added map and the NVSS map. Significance levels obtained from the 1000 Monte Carlo simulations are shown by the shaded regions for 68% (yellow), 95% (magenta) and 99% (red) levels.

- χ^2 test performed to compute significance of detections when all scales considered in aggregate
  - Signed-intensity: detection at 95% significance
  - Orientation: detection at 93% significance
  - Elongation: detection at 85% significance
- Foreground contamination and instrumental systematics ruled out as source of the correlation

Detections: Matched intensity correlation

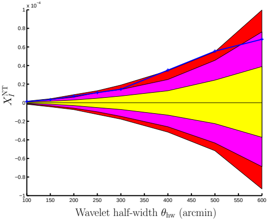

Figure: Correlation statistics computed for signed-intensity in the matched intensity analysis, from the WMAP co-added map and the NVSS map. Significance levels obtained from the 1000 Monte Carlo simulations are shown by the shaded regions for 68% (yellow), 95% (magenta) and 99% (red) levels.

- χ^2 test performed to compute significance of detection when all scales considered in aggregate
  - Signed-intensity: detection at 99.9% significance
- Foreground contamination and instrumental systematics ruled out as source of the correlation

Correlation by eye?

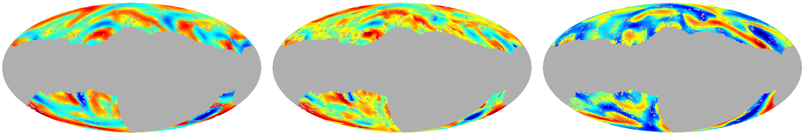

(a) WMAP for independent features (b) WMAP for features matched to NVSS orientations (c) NVSS

Figure: Morphological signed-intensity maps corresponding to the scale $(a = 400')$ on which the maximum detections of correlation are made. In panel (a) signed-intensities are shown for local features extracted independently from the WMAP co-added data, whereas in panel (b) signed-intensities are shown for local features in the WMAP co-added data that are matched in orientation to local features in the NVSS data. Due to the strength of the correlation in the data, it is possible to observe the correlation both between maps (a) and (c) and between maps (b) and (c) by eye.

Outline

Summary

- Correlation detected between the WMAP and NVSS data using all wavelet approachs
- Correlation signal consistent (in sign and scale) with predicted signal induced by ISW effect
- Foregrounds and systematics ruled out as the source of the correlation
- Positive detection of the ISW effect $\Rightarrow$ independent verification of dark energy
- ISW signal used to constrain properties of dark energy (in wavelet coefficient correlation case)

- Future work: use correlations detected in morphological analysis to constrain dark energy parameters (not trivial!)
- Future work: use detections to constrain properties of more sophisticated dark energy models that allow perturbations in the dark energy fluid

References

[1] N. Afshordi, Y.-S. Loh, and M. A. Strauss.
Cross-correlation of the cosmic microwave background with the 2MASS galaxy survey
Phys. Rev. D., D69:083524, 2004.

[2] J.-P. Antoine and P. Vandergheynst.
Wavelets on the n-sphere and related manifolds.
J. Math. Phys., 39(8):3987–4008, 1998.

[3] S. Boughn and R. Crittenden.
A correlation of the cosmic microwave sky with large scale structure.
Nature, 427:45–47, 2004.

[4] R. G. Crittenden and N. Turok.
Looking for Λ with the Rees-Sciama effect.
Phys. Rev. Lett., 76:575–578, 1996.

[5] J. D. McEwen, M. P. Hobson, D. J. Mortlock, and A. N. Lasenby.
Fast directional continuous spherical wavelet transform algorithms.
IEEE Trans. Sig. Proc., 55(2):520–529, 2007.

[6] J. D. McEwen, P. Vielva, M. P. Hobson, E. Martínez-González, and A. N. Lasenby.
Detection of the ISW effect and corresponding dark energy constraints made with directional spherical wavelets.
Mon. Not. Roy. Astron. Soc., 373:1211–1226, 2007.

[7] J. D. McEwen, Y. Wiaux, M. P. Hobson, P. Vandergheynst, and A. N. Lasenby.
Probing dark energy with steerable wavelets through correlation of WMAP and NVSS local morphological measures.
ArXiv, 2007.

[8] P. Vielva, E. Martínez-González, and M. Tucci.
Cross-correlation of the cosmic microwave background and radio galaxies in real, harmonic and wavelet spaces.
Mon. Not. Roy. Astron. Soc., 365:891–901, 2006.

[9] Y. Wiaux, L. Jacques, and P. Vandergheynst.
Correspondence principle between spherical and Euclidean wavelets.
Astrophys. J., 632:15–28, 2005.

[10] Y. Wiaux, L. Jacques, P. Vielva, and P. Vandergheynst.
Fast directional correlation on the sphere with steerable filters.
Astrophys. J., 652:820–832, 2006.